Pramana – J. Phys. (2018) 91:71
https://doi.org/10.1007/s12043-018-1643-9

Thermal transport of rate-type fluid impinging obliquely over a heated sheet

R MEHMOOD and S RANA*

Department of Mathematics, Faculty of Natural Sciences, HITEC University, Taxila Cantt, Pakistan
*Corresponding author. E-mail: srhtc2016@hotmail.com

MS received 2 November 2017; revised 13 April 2018; accepted 17 April 2018;
published online 20 September 2018

Abstract. The main objective of this study is to examine the two-dimensional (2D) oblique Oldroyd-B flow on a stretching heated sheet. The flow governing problem is converted into nonlinear ordinary differential equations through proper scaling transformations. The prevailing set of equations is solved computationally with a tolerance level of 10^{-5}. The velocity and temperature of a fluid model under consideration are portrayed to discuss the influence of all associated parameters on momentum and thermal characteristics. Heat flux at the wall has been computed numerically and analysed in a physical manner. The results obtained depict a reversed flow region for non-positive values of shear flow components once a free parameter is varied. It is noticed that heat transfer at the wall drops due to a rise in Deborah number β_1 as well as Biot number Bi.

Keywords. Oblique flow; heated sheet; Oldroyd-B fluid; numerical solution.

PACS Nos **44.25.+f; 47.10.ad; 47.50.−d**

1. Introduction

In the modern era, rheological fluids are most suitable and appropriate when compared with the ideal fluids due to their wide ranging applications in almost all fields of modern technology, for example in biology, medical science, pharmaceutical and chemical industries. All fluids that exist in nature, such as blood, mud, sauces, ketchup, shampoo, oil, paints, polymer solutions, clay coating, iron melting rods and many others are rheological fluids. These fluids are viscid and flexible under strain. The characteristics of all these types of rheological fluids can be described by highly nonlinear constitutive equations. In fact, Navier–Stokes theory does not completely define the rheological properties of complicated fluids. The major difficulty here is the presence of nonlinearity that cannot be handled by the traditional constitutive relation for all fluids. Camci and Herr [1] gave a detailed analysis of interactions of self-oscillation done on the impingement surface by taking into account thermal transport features. Mahapatra *et al* [2] studied heat transfer and thermal radiation of oblique flows. Tooke and Blyth [3] analysed an oblique stagnated stream using a free parameter and discussed shear flow with constant vorticity at infinity. Terzis *et al* [4] experimentally discovered the thermal inertia of a transient liquid crystal. Nawaz *et al* [5] studied the influence of joule heating of stagnated flow for both Newtonian and non-Newtonian models on a stretched cylinder. Crane [6] considered the fluid flow over a linear stretched sheet. Stretching flow along with thermal radiation under several physical constraints have been discussed in [7–13]. Various non-Newtonian fluid models have been suggested, which are mainly divided into three classes, namely rate-type, differential and integral-type. The Oldroyd-B model is an extension of the upper convected Maxwell model; it is a constitutive model that is used to describe the flow of viscoelastic fluids. This model is equivalent to a fluid filled with elastic beads and spring dumb-bells. In the dumb-bell model, the behaviour of a single polymer molecule in a fluid is considered, but this microscopic model does not describe the feedback effect that polymers have on the flow. To include the feedback effect, it is necessary to move onto a hydrodynamical description for the viscoelastic fluid. The Oldroyd-B model provides a simple linear viscoelastic model for dilute polymer solutions based on the dumb-bell model. The study on Oldroyd-B fluid is very limited in the past few years. Rajagopal and Bhatnagar [14] presented exact solutions for some modest streams of this model. Magyari and Keller [15] described a similar solution to the fluid on an

exponentially stretched sheet under power law boundary conditions and also discussed the effects of heat and mass transfer. Mompean and Deville [16] studied three-dimensional (3D) planar contraction of the unsteady Oldroyd-B coquette flow. Chen *et al* [17] discussed the case of unsteady state and unidirectional flow of an Oldroyd-B fluid in a circular duct, where fluid motion in the duct is influenced by the arbitrary inlet volume flow rate with time variation. Sajid *et al* [18] inspected the 2D Oldroyd-B fluid over a stretching sheet. Chen [19] derived a thin liquid film non-Newtonian fluid model with convective heat transfer characteristics along with viscid dissipation, and discussed velocity and temperature distribution for the free surface and for the wall as well. Qi and Jin [20] studied the unsteady helical flow of a generalised Oldroyd-B fluid between two infinite coaxial cylinders and within an infinite cylinder using a fractional calculus approach. Furthermore, Hailtao and Mingyu [21] provided analytical solutions to the unsteady unidirectional generalised Oldroyd-B fluid with a fractional derivative between two parallel plates. The literature on rheological fluids with and without manifestation of a magnetic field and convective heating has appeared to be advantageous in various technological and manufacturing procedures. Sajid *et al* [22] studied the steady mixed convective incompressible Oldroyd-B fluid with a constant magnetic field but with a variable temperature, which varies with distance. Zheng *et al* [23] presented the magnetohydrodynamics (MHD) flow of an incompressible generalised Oldroyd-B fluid induced by an accelerating plate, in which the no-slip assumption between the wall and the fluid is no longer valid and used fractional derivative for computations. Shehzad *et al* [24] described the thermophoretic MHD flow of the viscous fluid over an inclined surface with thermal radiation and heat generation. Nadeem *et al* [25] investigated numerical behaviour of the flow stream and the heat transmission of a rate-type fluid containing nanoparticles. Kuzentsov and Nield [26] studied natural convection of the nanofluid under the influence of Brownian motion and thermophoretic effects. Sheikholeslami *et al* [27] used a homogeneous model for simulation of H_2O single bond CuO nanofluid to eliminate the pressure gradient source terms and vorticity stream function. They also examined the effects of nanoparticles and Rayleigh number on flow characteristics. Sheikholeslami and Zeeshan [28] scrutinised the mesoscopic imitation of the nanofluid in porous medium with heat source. Sheikholeslami and Shamlooei [29] used $Fe_3O_4 - H_2O$ to explore the natural convection of radiative nanofluid. Bhatti and Rashidi [30] studied the influence of thermophoresis in combination with a radiative Williamson nanofluid. Some recent related studies on convection may be seen in [31–45].

All the previous studies have focussed on normal flow past a stretching sheet with various physical effects. The present model is novel and significant when compared with the previous studies as it examines an oblique stream of Oldroyd-B fluid past a stretching sheet under convective conditions. To the best of our knowledge, the oblique flow of an Oldroyd-B-type fluid over a convective surface has never been addressed before. The outcome of this study can be considered as a benchmark for certain industrial applications.

2. Mathematical modelling and assumptions

The constitutive equations of an Oldroyd-B fluid are as follows [45]:

$$T = -pI + S, \tag{1}$$

where T is the Cauchy stress tensor, p is the pressure term, I is the identity, S is the extra stress tensor, defined by

$$S + \lambda_1 \left(\frac{\mathrm{D}S}{\mathrm{D}t} - LS - SL^{\mathrm{T}} \right) = \mu \left(A_1 + \lambda_2 \left(\frac{\mathrm{D}A_1}{\mathrm{D}t} - LA_1 - A_1 L^{\mathrm{T}} \right) \right), \tag{2}$$

where μ is the dynamic viscosity, λ_1 is the ratio of relaxation to retardation times, λ_2 is the retardation time, $\mathrm{D}/\mathrm{D}t$ is the material derivative defined by

$$\left(\frac{\mathrm{D}}{\mathrm{D}t} \right) = \left(\frac{\partial}{\partial t} \right) + V \cdot \nabla. \tag{3}$$

A_1 is the first Rivilin Ericksen tensor defined by

$$A_1 = \nabla V + (\nabla V)^t = L + L^{\mathrm{T}}. \tag{4}$$

For the present problem under consideration, a steady 2D incompressible Oldroyd-B fluid flowing on the stretching sheet is taken after assuming that the fluid meets the wall at an oblique manner. The surface is assumed to be convective due to the presence of a hot fluid beneath the surface. To maintain balance, the wall is stretched by keeping the original static equilibrium balanced force imposed on the x-direction (see figure 1). The basic equations of continuity, x and y momentum equations along with an energy equation for this Oldroyd-B model are as follows [3,44]:

$$\frac{\partial u}{\partial x} + \frac{\partial v}{\partial y} = 0, \tag{5}$$

$$u\frac{\partial u}{\partial x} + v\frac{\partial u}{\partial y} + \frac{1}{\rho}\frac{\partial p}{\partial x} + \lambda_1 \left(u^2 \frac{\partial^2 u}{\partial x^2} + v^2 \frac{\partial^2 u}{\partial y^2} + 2uv \frac{\partial^2 u}{\partial x \partial y} \right)$$

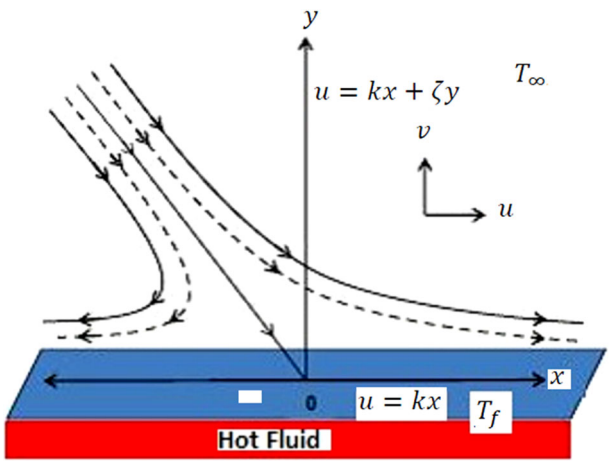

Figure 1. Physical representation of the fluid model.

$$= \nu\left[\frac{\partial^2 u}{\partial x^2} + \frac{\partial^2 u}{\partial y^2} + \lambda_2\left(u\frac{\partial^3 u}{\partial x^3} + u\frac{\partial^3 u}{\partial x \partial y^2} + v\frac{\partial^3 u}{\partial y^3} + v\frac{\partial^3 u}{\partial y \partial x^2} - \frac{\partial u}{\partial x}\frac{\partial^2 u}{\partial x^2} - \frac{\partial u}{\partial x}\frac{\partial^2 u}{\partial y^2} - \frac{\partial u}{\partial y}\frac{\partial^2 v}{\partial x^2} - \frac{\partial u}{\partial y}\frac{\partial^2 v}{\partial y^2}\right)\right], \tag{6}$$

$$u\frac{\partial v}{\partial x} + v\frac{\partial v}{\partial y} + \frac{1}{\rho}\frac{\partial p}{\partial y} + \lambda_1\left(u^2\frac{\partial^2 v}{\partial x^2} + v^2\frac{\partial^2 v}{\partial y^2} + 2uv\frac{\partial^2 v}{\partial x \partial y}\right) = \nu\left[\frac{\partial^2 v}{\partial x^2} + \frac{\partial^2 v}{\partial y^2} + \lambda_2\left(u\frac{\partial^3 v}{\partial x^3} + u\frac{\partial^3 v}{\partial x \partial y^2} + v\frac{\partial^3 v}{\partial y^3} + v\frac{\partial^3 v}{\partial y \partial x^2} - \frac{\partial v}{\partial x}\frac{\partial^2 u}{\partial x^2} - \frac{\partial v}{\partial x}\frac{\partial^2 u}{\partial y^2} - \frac{\partial v}{\partial y}\frac{\partial^2 v}{\partial x^2} - \frac{\partial y}{\partial \bar{x}_2}\frac{\partial^2 v}{\partial y^2}\right)\right], \tag{7}$$

$$u\frac{\partial T}{\partial x} + v\frac{\partial T}{\partial y} = \alpha\left(\frac{\partial^2 T}{\partial x^2} + \frac{\partial^2 T}{\partial y^2}\right). \tag{8}$$

Following Tooke and Blyth [3]

$$\left.\begin{aligned} &u = kx, v = 0,\\ &-k_1\frac{\partial T}{\partial y} = h\left(T_f - T\right) \text{ at } y = 0,\\ &u = kx + \zeta y,\\ &T = T_\infty \text{ at } y \to \infty. \end{aligned}\right\} \tag{9}$$

Here u is considered to be the x-component and v is considered to be the y-component of velocity, ν is the effective kinematic viscosity, p is the pressure, ρ is the density, T is the temperature, λ_1 and λ_2 are the relaxation and retardation times, k_1 is the thermal conductivity, α is the thermal diffusivity, T_∞ is the ambient fluid temperature and k is the strength of the irrotational straining flow. The wall is taken to be parallel to the x-axis and the fluid is considered within the region $y > 0$. Define stream function $\psi(x, y)$ along with velocity [3]:

$$u = \frac{\partial \psi}{\partial y}, v = -\frac{\partial \psi}{\partial x}. \tag{10}$$

Away from the wall, the flow is given by [3]

$$\psi(x, y) = kxy + \frac{1}{2}\zeta y^2, \tag{11}$$

where k is the strength of an irrotational straining flow and ζ is the vorticity of a rotating shear flow in the x-direction.

Using eq. (10), eq. (5) is identically satisfied and the set of eqs (6)–(9) takes the form:

$$\frac{\partial \psi}{\partial y}\frac{\partial^2 \psi}{\partial x \partial y} - \frac{\partial \psi}{\partial x}\frac{\partial^2 \psi}{\partial y^2} + \frac{1}{\rho}\frac{\partial p}{\partial x} + \lambda_1\left(\left(\frac{\partial \psi}{\partial y}\right)^2\frac{\partial^3 \psi}{\partial x^2 \partial y} + \left(\frac{\partial \psi}{\partial x}\right)^2\frac{\partial^3 \psi}{\partial y^3} - 2\frac{\partial \psi}{\partial y}\frac{\partial \psi}{\partial x}\frac{\partial^3 \psi}{\partial x \partial y^2}\right) = \nu\left[\frac{\partial^3 \psi}{\partial x^2 \partial y} + \frac{\partial^3 \psi}{\partial y^3} + \lambda_2\left(\frac{\partial \psi}{\partial y}\frac{\partial^4 \psi}{\partial x^3 \partial y} + \frac{\partial \psi}{\partial y}\frac{\partial^4 \psi}{\partial x^2 \partial y^2} - \frac{\partial \psi}{\partial x}\frac{\partial^4 \psi}{\partial y^3} - \frac{\partial \psi}{\partial x}\frac{\partial^4 \psi}{\partial y^4} - \frac{\partial^2 \psi}{\partial x \partial y}\frac{\partial^3 \psi}{\partial x^2 \partial y} - \frac{\partial^2 \psi}{\partial x \partial y}\frac{\partial^3 \psi}{\partial y^3} - \frac{\partial^2 \psi}{\partial y^2}\frac{\partial^3 \psi}{\partial x^2 \partial y} + \frac{\partial^2 \psi}{\partial y^2}\frac{\partial^3 \psi}{\partial y^2 \partial x}\right)\right], \tag{12}$$

$$\frac{\partial \psi}{\partial y}\frac{\partial^2 \psi}{\partial x^2} + \frac{\partial \psi}{\partial x}\frac{\partial^2 \psi}{\partial x \partial y} + \frac{1}{\rho}\frac{\partial p}{\partial y} + \lambda_1\left(-\left(\frac{\partial \psi}{\partial y}\right)^2\frac{\partial^3 \psi}{\partial x^3} - \left(\frac{\partial \psi}{\partial x}\right)^2 \times \frac{\partial^3 \psi}{\partial x \partial y^2} + 2\frac{\partial \psi}{\partial y}\frac{\partial \psi}{\partial x}\frac{\partial^3 \psi}{\partial y \partial x^2}\right) = \nu\left[-\frac{\partial^3 \psi}{\partial x^3} - \frac{\partial^3 \psi}{\partial x \partial y^2} + \lambda_2\left(-\frac{\partial \psi}{\partial y}\frac{\partial^4 \psi}{\partial x^4} - \frac{\partial \psi}{\partial y}\frac{\partial^4 \psi}{\partial x^2 \partial y^2} + \frac{\partial \psi}{\partial x}\frac{\partial^4 \psi}{\partial x^3 \partial y} + \frac{\partial \psi}{\partial x}\frac{\partial^4 \psi}{\partial x \partial y^3} + \frac{\partial^2 \psi}{\partial x^2}\frac{\partial^3 \psi}{\partial x^2 \partial y} + \frac{\partial^2 \psi}{\partial x^2}\frac{\partial^3 \psi}{\partial y^3}\right)\right]$$

$$-\frac{\partial^3\psi}{\partial x^3}\frac{\partial^2\psi}{\partial x\partial y}-\frac{\partial^2\psi}{\partial x\partial y}\frac{\partial^3\psi}{\partial x\partial y^2}\Bigg)\Bigg], \tag{13}$$

$$\frac{\partial\psi}{\partial y}\frac{\partial T}{\partial x}-\frac{\partial\psi}{\partial x}\frac{\partial T}{\partial y}=\alpha\left(\frac{\partial^2 T}{\partial x^2}+\frac{\partial^2 T}{\partial y^2}\right). \tag{14}$$

The consistent boundary conditions are taken as follows:

$$\begin{aligned}&\frac{\partial\psi}{\partial y}=kx,\quad -\frac{\partial\psi}{\partial x}=0,\\ &-k_1\frac{\partial T}{\partial y}=h\big(T_f-T\big)\quad \text{at } y=0,\\ &\frac{\partial\psi}{\partial y}=kx+\zeta y,\quad \frac{\partial\psi}{\partial x}=0,\\ &T=T_\infty\quad \text{as } y\to\infty.\end{aligned} \tag{15, 16}$$

Now by removing the pressure term and by using $p_{xy}=p_{yx}$, we obtain the following set of equations:

$$\begin{aligned}&\frac{\partial\psi}{\partial y}\left(\frac{\partial^3\psi}{\partial x\partial y^2}+\frac{\partial^3\psi}{\partial x^3}\right)\\ &-\frac{\partial\psi}{\partial x}\left(\frac{\partial^3\psi}{\partial y\partial x^2}+\frac{\partial^3\psi}{\partial y^3}\right)+\lambda_1\Bigg[2\frac{\partial^3\psi}{\partial x^2\partial y}\left(\frac{\partial\psi}{\partial y}\frac{\partial^2\psi}{\partial y^2}\right.\\ &\left.-\frac{\partial\psi}{\partial x}\frac{\partial^2\psi}{\partial x\partial y}-\frac{\partial\psi}{\partial y}\frac{\partial^2\psi}{\partial x^2}\right)\\ &+2\frac{\partial^2\psi}{\partial x\partial y}\left(\frac{\partial\psi}{\partial x}\frac{\partial^3\psi}{\partial y^3}+\frac{\partial\psi}{\partial y}\frac{\partial^3\psi}{\partial x^3}\right)\\ &+2\frac{\partial^3\psi}{\partial x\partial y^2}\left(-\frac{\partial^2\psi}{\partial y^2}\frac{\partial\psi}{\partial x}+\frac{\partial\psi}{\partial x}\frac{\partial^2\psi}{\partial x^2}-\frac{\partial\psi}{\partial y}\frac{\partial^2\psi}{\partial x\partial y}\right)\\ &+\frac{\partial^4\psi}{\partial x^2\partial y^2}\left(\left(\frac{\partial\psi}{\partial y}\right)^2+\left(\frac{\partial\psi}{\partial x}\right)^2\right)\\ &+\left(\frac{\partial\psi}{\partial x}\right)^2\frac{\partial^4\psi}{\partial y^4}-2\frac{\partial\psi}{\partial x}\frac{\partial\psi}{\partial y}\frac{\partial^4\psi}{\partial x\partial y^3}\\ &+\left(\frac{\partial\psi}{\partial y}\right)^2\frac{\partial^4\psi}{\partial x^4}-2\frac{\partial\psi}{\partial x}\frac{\partial\psi}{\partial y}\frac{\partial^4\psi}{\partial y\partial x^3}\Bigg]\\ &-\nu\Bigg[\nabla^4\psi+\lambda_2\Bigg(-2\frac{\partial^2\psi}{\partial x\partial y}\nabla^4\psi+\frac{\partial^2\psi}{\partial y^2}\left(\frac{\partial^4\psi}{\partial y\partial x^3}\right.\\ &\left.+2\frac{\partial^4\psi}{\partial x\partial y^3}-\frac{\partial^4\psi}{\partial x^2\partial y^2}\right)\\ &+\frac{\partial\psi}{\partial y}\left(\frac{\partial^5\psi}{\partial y^2\partial x^3}+\frac{\partial^5\psi}{\partial x\partial y^4}+\frac{\partial^5\psi}{\partial x^5}+\frac{\partial^5\psi}{\partial x^3\partial y^2}\right)\\ &+\frac{\partial\psi}{\partial x}\left(-\frac{\partial^5\psi}{\partial y^2\partial x^3}-\frac{\partial^5\psi}{\partial y\partial x^4}-\frac{\partial^5\psi}{\partial y^5}-\frac{\partial^5\psi}{\partial y^3\partial x^2}\right)\\ &-2\frac{\partial^2\psi}{\partial x^2}\left(\frac{\partial^4\psi}{\partial y\partial x^3}+\frac{\partial^4\psi}{\partial x\partial y^3}\right)\end{aligned}$$

$$-\frac{\partial^3\psi}{\partial y^3}\left(\frac{\partial^3\psi}{\partial x^3}+\frac{\partial^3\psi}{\partial y\partial x^2}\right)\Bigg)\Bigg]=0, \tag{17}$$

$$\frac{\partial\psi}{\partial y}\frac{\partial T}{\partial x}-\frac{\partial\psi}{\partial x}\frac{\partial T}{\partial y}=\alpha\left(\frac{\partial^2 T}{\partial x^2}+\frac{\partial^2 T}{\partial y^2}\right). \tag{18}$$

Along with the boundary conditions

$$\left.\begin{aligned}&\frac{\partial\psi}{\partial y}=kx,-\frac{\partial\psi}{\partial x}=0,\\ &-k_1\frac{\partial T}{\partial y}=h\big(T_f-T\big),\end{aligned}\right\}\ \text{at } y=0, \tag{19}$$

$$\left.\begin{aligned}&\frac{\partial\psi}{\partial y}=kx+\zeta y,\\ &\frac{\partial\psi}{\partial x}=0,\ T=T_\infty,\end{aligned}\right\}\ \text{at } y=\infty. \tag{20}$$

Adjacent to the wall, let us pursue a solution in general form, by redefining the stream function as [3]

$$\psi=\sqrt{\upsilon k}xf(\eta)+\zeta\left(\frac{\upsilon}{k}\right)\int_0^\eta g(t)\mathrm{d}t,\quad \theta=\frac{T-T_\infty}{T_f-T_\infty}, \tag{21}$$

where $\eta=\sqrt{(k/\nu)}y$.

Using eq. (21) in (17)–(20) and integrating the resultant equation one time for simplification, we obtain

$$\begin{aligned}&f'''+ff''-(f')^2+\beta_1(2ff'f''-f^2f''')\\ &+\beta_2(f''^2-ff'''')+B_1=0,\end{aligned} \tag{22}$$

$$\begin{aligned}&g''-gf'+fg'+\beta_1\left(2fgf''-f^2g''\right)\\ &+\beta_2(f''g'+f''g'-f'g''-fg''')+B_2=0,\end{aligned} \tag{23}$$

$$\theta''+\ \mathrm{Pr}f\theta'=0, \tag{24}$$

and boundary conditions (19) and (20) take the following forms:

$$\left.\begin{aligned}&f=0,\ f'=0,\\ &g=0,\ g'=0,\\ &\theta'=-\ \mathrm{Bi}(1-\theta(0))\ ,\end{aligned}\right\}\ \text{at } \eta=0, \tag{25}$$

$$\left.\begin{aligned}&f'=1,\ g'=1,\\ &\theta=0,\end{aligned}\right\}\ \text{at } \eta\to\infty. \tag{26}$$

Steadiness with free stream flow implies approximately [3]

$$f(\eta)=\eta-\alpha,\quad g(\eta)=\eta-\beta\quad \text{as } \eta\to\infty,$$

where α and β are constants, $\beta_1=\lambda_1 a$ and $\beta_2=\lambda_2 a$ are the Deborah numbers, $\mathrm{Pr}=(\nu/\alpha)$ is the Prandtl number, $\mathrm{Bi}=-(h/k_1)\sqrt{\nu/k}$ is the Biot number. Applying boundary conditions (26) at infinity in eqs (22) and (23), we obtain

$$B_1 = 1, \quad B_2 = -(\alpha - \beta), \tag{27}$$

where α and β are constants.

Using eq. (27) in eqs (22) and (23) give

$$f''' + ff'' - (f')^2 + \beta_1(2ff'f'' - f^2 f''') + \beta_2(f''^2 - ff'''') + 1 = 0, \tag{28}$$

$$g'' - f'g + fg' + \beta_1(2fgf'' - f^2 g'') + \beta_2(f'''g + f''g' - f'g'' - fg''') - (\alpha - \beta) = 0, \tag{29}$$

$$\theta'' + \Pr f\theta' = 0. \tag{30}$$

Along with the boundary conditions

$$f(0) = 0, \quad f'(0) = 1, \quad g(0) = 0,$$

$$\theta'(0) = -\mathrm{Bi}(1 - \theta(0)), \tag{31}$$

$$f'(\infty) = \frac{a}{k}, \quad g'(\infty) = 1, \quad \theta(\infty) = 0. \tag{32}$$

In the above relations, prime signifies derivatives with respect to η.

3. Concerned physical magnitudes

The practical physical quantity of interest is the heat transfer rate at the convective surface, which is defined as

$$z_w = -k\left(\frac{\partial T}{\partial y}\right) \text{ at } y = 0. \tag{33}$$

In the non-dimensional form

$$z_w = -\theta'(0). \tag{34}$$

4. Numerical computation

The governed model of eqs (28)–(30) and relevant boundary conditions (31) and (32) are nonlinear in nature. So, it must be tackled with some computational strategy. This governed model is first converted into a scheme of nonlinear ordinary differential equations of order one. With the aid of a computational technique for solving an initial value problem, known to be the Runge–Kutta method of order five, along with a shooting technique, a concerned system is solved as follows.

Define the following new scheme in eqs (28)–(32):

$$\left.\begin{aligned} &\begin{pmatrix} f = y_1 \\ f' = y_1' = y_2 \\ f'' = y_2' = y_3 \\ f''' = y_3' = y_4 \\ f'''' = y_4' = y_5 \end{pmatrix} \\ &\begin{pmatrix} g = y_6 \\ g' = y_6' = y_7 \\ g'' = y_7' = y_8 \\ g''' = y_8' = y_9 \end{pmatrix} \\ &\begin{pmatrix} \theta = y_{10} \\ \theta' = y_{10}' = y_{11} \\ \theta'' = y_{11}' = y_{12} \end{pmatrix} \end{aligned}\right\}. \tag{35}$$

We obtain the following system of the initial value problem:

$$y_1 y_4' = \frac{1}{\beta_2}\left[y_4 + y_1 y_3 - y_2^2 + \beta_1\left\{2y_1 y_2 y_3 - y_4 y_1^2\right\} + 1\right] + y_3^2, \tag{36}$$

$$y_1 y_8' = \frac{1}{\beta_2}\left[y_8 + y_1 y_7 - y_2 y_6 + \beta_1\left\{2y_1 y_3 y_6 - y_8 y_1^2\right\} - (\alpha - \beta)\right] + y_4 y_6 + y_3 y_7 - y_2 y_8, \tag{37}$$

$$y_{11}' = -\Pr\ y_1 y_{11}, \tag{38}$$

$$\left.\begin{aligned} &y_1(0) = 0,\ y_3(0) = 0, \\ &y_4(0) = \alpha_1,\ y_6(0) = 0, \\ &y_8(0) = \alpha_2,\ y_8(0) = \alpha_3, \\ &y_{11}(0) = \alpha_4, \end{aligned}\right\} \tag{39}$$

where $\alpha_1, \alpha_2, \alpha_3$ and α_4 are shooting constraints. A suitable tolerance level of 10^{-5} is taken in all computations.

5. Theoretical discussion

Extensive computations have been conducted using the shooting quadrature technique in this section. The velocity, temperature and surface heat flux of the fluid for all governed parameters are explored through figures 2–15. Figures 2 and 3 exhibit the behaviour of a normal component of velocity for Deborah numbers β_1 and β_2. We observe that with an increase in Deborah number β_1, normal velocity $f'(\eta)$ and momentum boundary layer thickness increases while it decreases with an increase in Deborah number β_2.

Figures 4 and 5 are plotted to inspect the tangential velocity $g'(\eta)$ against Deborah numbers β_1 and β_2. An enhancement in Deborah numbers β_1 and β_2 depicts that velocity $g'(\eta)$ accelerates close to the wall but reverses its behaviour away from the wall. Deborah numbers

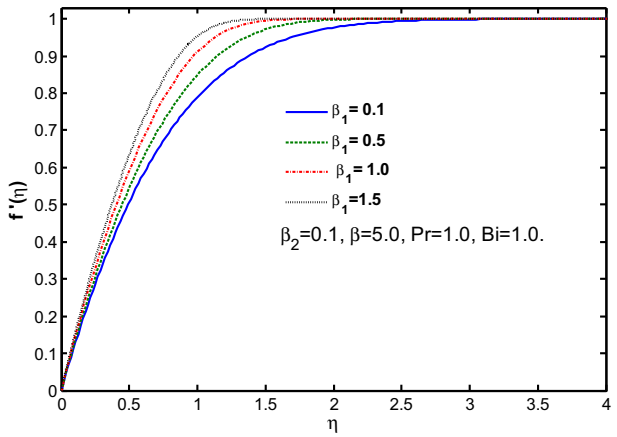

Figure 2. Normal velocity $f'(\eta)$ for $\beta_1 = 0.1, 0.5, 1.0$ and 1.5.

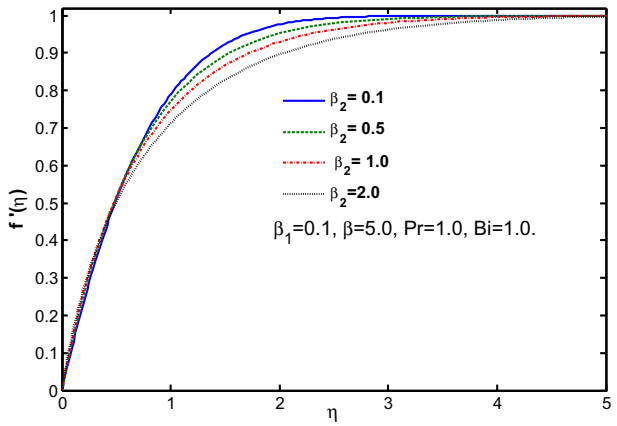

Figure 3. Normal velocity $f'(\eta)$ for $\beta_2 = 0.1, 0.5, 1.0$ and 2.0.

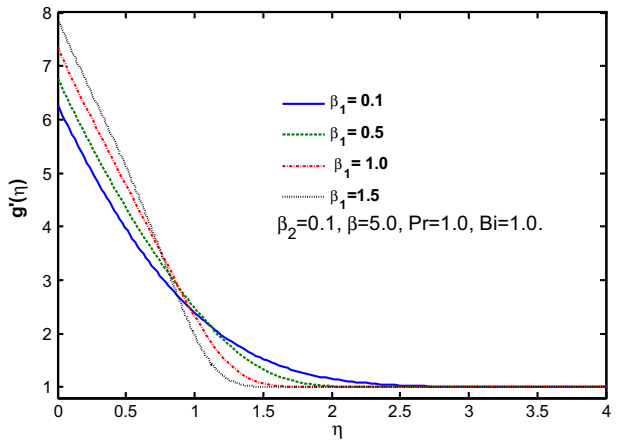

Figure 4. Shear velocity $g'(\eta)$ for $\beta_1 = 0.1, 0.5, 1.0$ and 1.5.

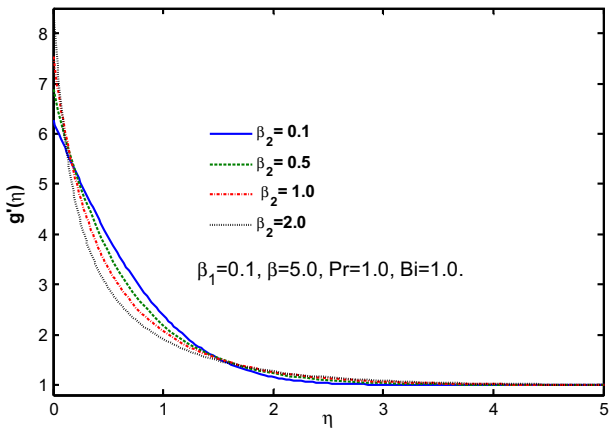

Figure 5. Shear velocity $g'(\eta)$ for $\beta_2 = 0.1, 0.5, 1.0$ and 2.0.

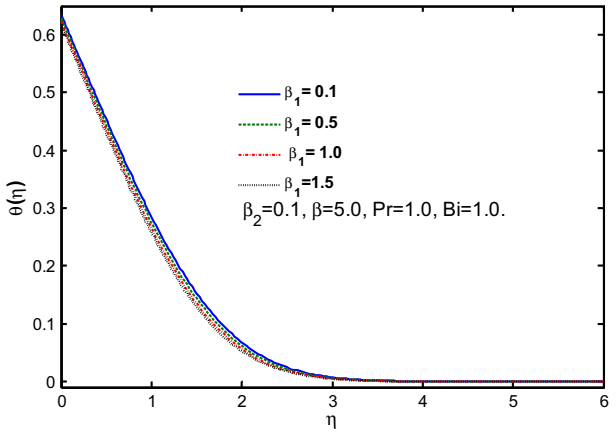

Figure 6. Temperature $\theta(\eta)$ for $\beta_1 = 0.1, 0.5, 1.0$ and 1.5.

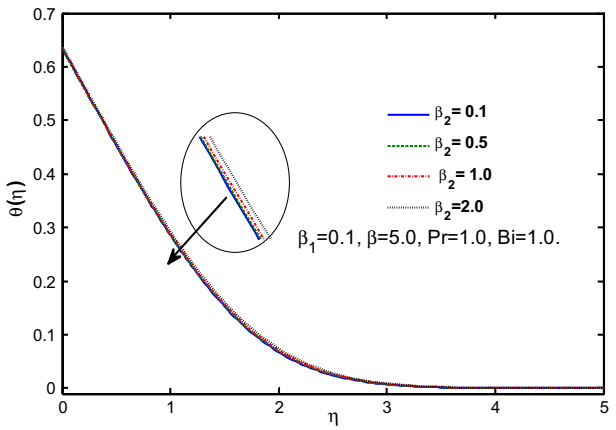

Figure 7. Temperature $\theta(\eta)$ for $\beta_2 = 0.1, 0.5, 1.0$ and 2.0.

are associated with the relaxation time phenomenon for certain rheological fluids which reflect the time taken by materials to regulate against applied stresses comprising elastic as well as viscous properties of the material. At small Deborah numbers, materials exhibit a fluid-like response, gradually changing the trend to solid-like response with larger Deborah numbers. Smaller Deborah number fluids neglect elastic

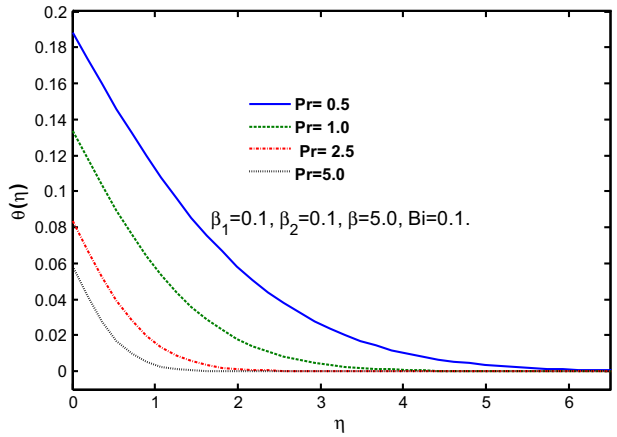

Figure 8. Temperature $\theta(\eta)$ for Pr $= 0.5$, 1.0, 2.5 and 5.0.

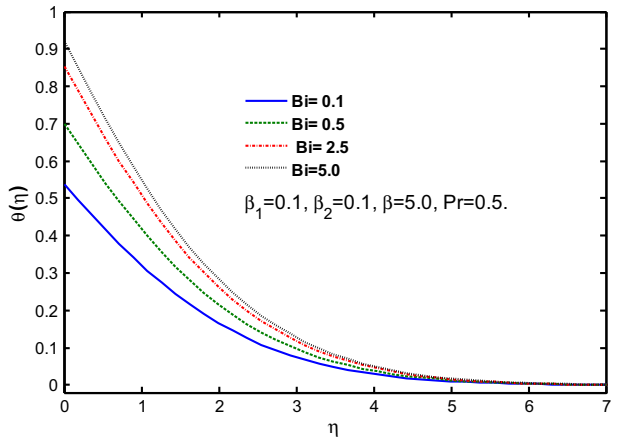

Figure 9. Temperature $\theta(\eta)$ for Bi $= 0.1$, 0.5, 2.5 and 5.0.

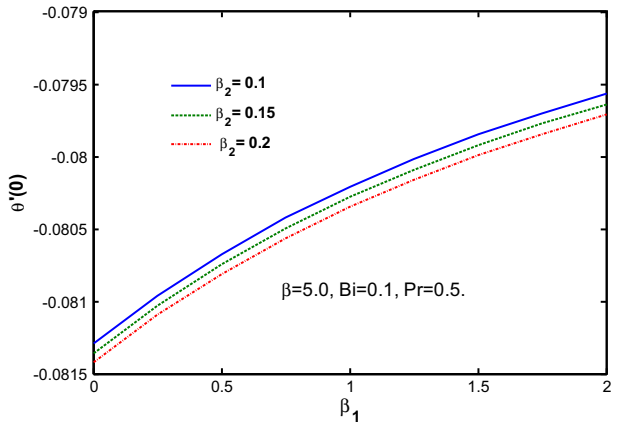

Figure 10. $\theta'(0)$ against Deborah number β_1 for $\beta_2 = 0.1$, 0.15 and 0.2.

properties, which result in acceleration of normal velocity while generating tangential momentum. Higher Deborah number means greater relaxation time which leads to the deceleration of normal velocity.

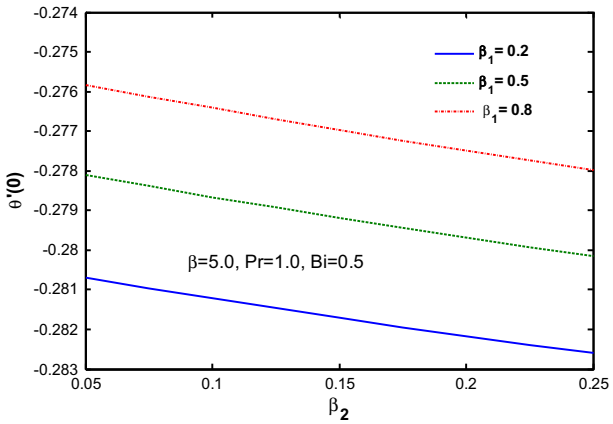

Figure 11. $\theta'(0)$ against Deborah number β_2 for $\beta_1 = 0.2$, 0.5 and 0.8.

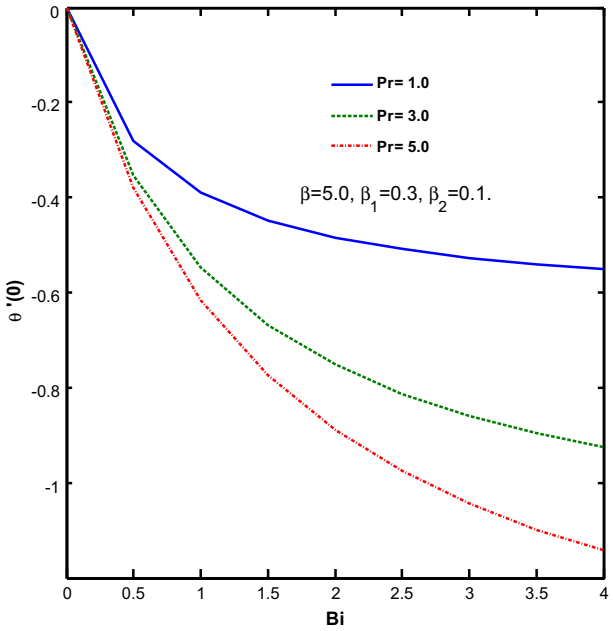

Figure 12. $\theta'(0)$ against Biot number Bi when Pr $= 1.0$, 3.0 and 5.0.

Figures 6–9 are plotted to explore the temperature profile $\theta(\eta)$ against emerging physical parameters such as Deborah numbers β_1 and β_2, Biot number Bi and Prandtl number Pr. From figure 6, we find that the temperature of the fluid and thermal boundary layer tend to decline for Deborah number β_1, but for Deborah number β_2, temperature and thermal boundary layer thickness increase as shown in figure 7. It can be observed from figure 8 that for Prandtl number Pr, temperature $\theta(\eta)$ and thermal boundary layer thickness of fluid diminishes. The physical justification for this response is that smaller Prandtl number fluids are more conductive compared to higher Prandtl number fluids and so with increasing Prandtl number

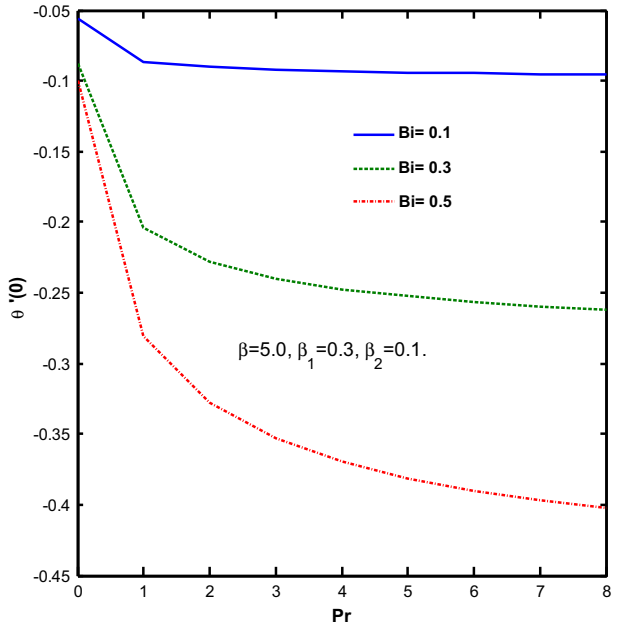

Figure 13. $\theta'(0)$ against Prandtl number Pr when Bi $= 0.1$, 0.3 and 0.5.

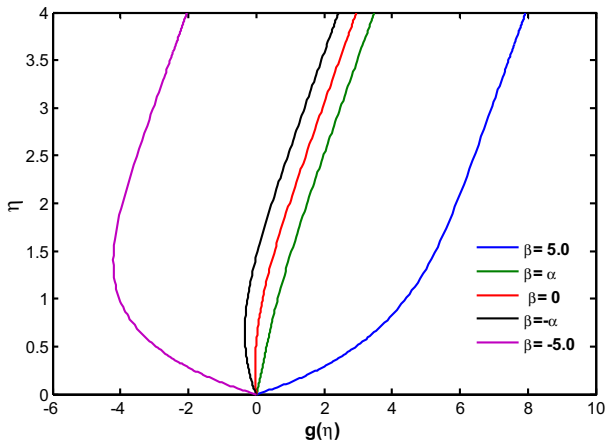

Figure 14. Shear flow component $g(\eta)$ for $\beta = 5.0, \alpha, 0, -\alpha, -5.0$.

thermal diffusion decreases which enhances the momentum diffusion, thus leading to the acceleration of the flow from the wall.

Figure 9 shows that the temperature and the corresponding thermal boundary layer increase with an increase in Biot number Bi. Biot number is directly related to heat transfer coefficient, whereas it is inversely related to thermal conductivity. That is, larger Biot number indicates low thermal conductivity.

Figures 10–13 are plotted to inspect local heat transfer coefficient $\theta'(0)$ against various parameters such as Deborah numbers β_1 and β_2, Biot number Bi and Prandtl number Pr. Figure 10 shows that heat flux at the wall $\theta'(0)$ increases significantly with an increase

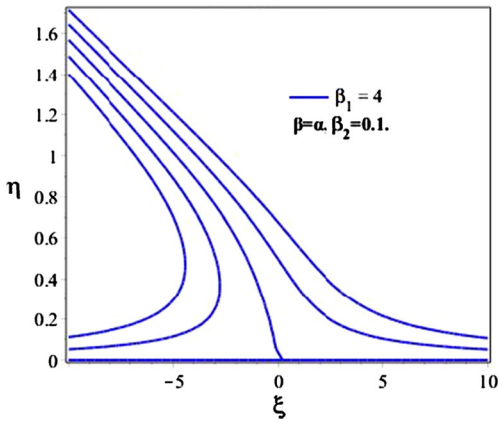

Figure 15. Stream lines pattern for Deborah numbers $\beta_1 = 4.0$, with $k/\zeta = 1/6$.

in Deborah number β_1 while from figure 11 it is quite evident that local heat flux drops with Deborah number β_2. Figures 12 and 13 reveal that heat flux at the wall decreases significantly with an increase in Biot number Bi and Prandtl number Pr. This follows from the fact that with larger Biot number, the ability of the fluid to conduct heat reduces significantly which causes a deceleration in the heat transfer rate at the convective sheet.

Figure 14 is plotted to express the shear flow component $g(\eta)$. It is quite clear from this figure that for different values of constant β, there is a distinct region of reversed flow corresponding to negative values of g. Figure 15 is plotted to explore the flow pattern with Deborah number β_1 for obliqueness $(k/\zeta) = 1/6$. The stream contour $\psi = 0$ touches the partition $\eta = 0$ at abscissa $\xi = \sqrt{(k/v)}x$. It is quite evident from this figure that the streamline patterns of the Oldroyd-B fluid are negatively skewed with a positive contribution of the Deborah number β_1.

6. Concluding remarks

The present numerical study is conducted to explore the 2D oblique stream of an Oldroyd-B-type fluid over a stretching sheet. Thermal effects on the sheet are incorporated under convective boundary conditions.

Major results of this study can be summarised as follows: normal velocity profile $f'(\eta)$ increases with Deborah number β_1. An increment in Deborah number β_1 shrinks momentum boundary layer thickness while it augments the thermal boundary layer thickness. Tangential velocity $g'(\eta)$ surges up close to the wall while reverses its behaviour far away from the wall with Deborah number β_1. Heat flux at the convective surface is decelerated with all associated parameters namely

Deborah numbers β_1 and β_2. The physical boundary layer displacement constant β generates a distinct region of reversed flow corresponding to the negative values of shear flow component g. Streamline patterns are negatively skewed with positive contribution of the Deborah number β_1.

References

[1] C Camci and F Herr, *ASME J. Heat Transfer* **124**(**4**), 770 (2002)
[2] T R Mahapatra, S K Nandy and A S Gupta, *MECC* **47**(**6**), 1325 (2012)
[3] R Tooke and M Blyth, *Phys. Fluids* **20**(**3**), 033101 (2008)
[4] A Terzis, V W Jens, W Bernhard and O Peter, *Meas. Sci. Tech.* **23**(**11**), 115303 (2012)
[5] M Nawaz, A Zeeshan, R Ellahi, S Abbasbandy and S Rashidi, *Int. J. Numer. Methods Fluids* **25**(**3**), 665 (2015)
[6] L J Crane, *Z. Angew. Math. Phys.* **21**(**4**), 645 (1970)
[7] R Cortell, *Int. J. Nonlinear Mech.* **41**(**1**), 78 (2006)
[8] M M Bhatti, T Abbas, M M Rashidi and M S Ali, *Entropy* **18**(**6**), 200 (2016)
[9] M M Bhatti, T Abbas, M M Rashidi, M S Ali and Y Zhigang, *Entropy* **18**(**6**), 224 (2016)
[10] S Mishra, P K Pattnaik, M M Bhatti and T Abbas, *Ind. J. Phys.* **91**(**10**), 1219 (2017)
[11] M M Bhatti, M M Rashidi and I Pop, *Nonlinear Eng.* **6**(**1**), 43 (2017)
[12] M M Bhatti, T Abbas and M M Rashidi, *Multidiscip. Model. Mater. Struct.* **12**(**4**), 605 (2016)
[13] M Sheikholeslami and M M Bhatti, *Int. J. Heat Mass Transfer* **111**, 1039 (2017)
[14] K Rajagopal and R Bhatnagar, *Acta Mech.* **113**(**1–4**), 233 (1995)
[15] E Magyari and B Keller, *J. Phys. D* **32**(**5**), 577 (1999)
[16] G Mompean and M Deville, *J. Non-Newtonian Fluid Mech.* **72**(**2–3**), 253 (1997)
[17] C I Chen, C K Chen and Y T Yang, *Heat Mass Transfer* **40**(**3–4**), 203 (2004)
[18] M Sajid, Z Abbas, T Javed and N Ali, *Can. J. Phys.* **88**(**9**), 635 (2010)
[19] C H Chen, *J. Non-Newtonian Fluid Mech.* **135**(**2–3**), 128 (2006)
[20] H Qi and H Jin, *Nonlinear Anal. Real World Appl.* **10**(**5**), 2700 (2009)
[21] Q Haitao and X Mingyu, *Appl. Math. Model.* **33**(**11**), 4184 (2009)
[22] M Sajid, B Ahmed and Z Abbas, *J. Egypt. Math. Soc.* **23**(**2**), 440 (2015)
[23] L Zheng, Y Liu and X Zhang, *Nonlinear Anal. Real World Appl.* **13**(**2**), 513 (2012)
[24] S A Shehzad, A Alsaedi, T Hayat and M S S Alhuthali, *J. Taiwan Inst. Chem. Eng.* **45**(**3**), 787 (2014)
[25] S Nadeem, R U Haq, N S Akbar, C Lee and Z H Khan, *PLoS ONE* **8**(**8**), 69811 (2013)
[26] A Kuznetsov and D Nield, *Int. J. Therm. Sci.* **49**(**2**), 243 (2010)
[27] M Sheikholeslami, M Nimafar, D D Ganji and M Pouyandehmehr, *Int. J. Hydrogen Energy* **41**(**40**), 17837 (2016)
[28] M Sheikholeslami and A Zeeshan, *Int. J. Hydrogen Energy* **42**(**22**), 15393 (2017)
[29] M Sheikholeslami and M Shamlooei, *Int. J. Hydrogen Energy* **42**(**9**), 5708 (2017)
[30] M M Bhatti and M M Rashidi, *J. Mol. Liq.* **221**, 567 (2016)
[31] O D Makinde and A Aziz, *Int. J. Therm. Sci.* **49**(**9**), 1813 (2010)
[32] G Swapna, K Lokendra, P Rana and B Singh, *J. Taiwan Inst. Chem. Eng.* **47**, 18 (2015)
[33] W Ibrahim and O D Makinde, *J. Aerosp. Eng.* **29**(**2**), 04015037 (2015)
[34] M Rahman, T Grosan, V Alin and I Pop, *Int. J. Numer. Methods Fluids* **25**(**2**), 299 (2015)
[35] A Malvandi, F Hedayati and D D Ganji, *J. Appl. Fluid Mech.* **8**(**1**), 151 (2015)
[36] D Kalidas, D P Ranjan and K P Kumar, *J. Egypt. Math. Soc.* **23**(**2**), 435 (2015)
[37] R Kandasamy, C Jeyabalan and K K S Prabhu, *Appl. Nanosci.* **6**(**2**), 287 (2016)
[38] S M Mamourian, K Milani, R Ellahi and A B Rahimi, *Int. J. Heat Mass Transfer* **102**, 544 (2016)
[39] S Rashidi, J A Esfahani and R Ellahi, *J. Appl. Sci.* **7**(**4**), 431 (2017)
[40] M Sheikholeslami, R Ellahi and K Vafai, *Alexandria Eng. J.* https://doi.org/10.1016/j.aej.2017.01.027 (2017)
[41] A Zeeshan, N Shehzad, R Ellahi and S Z Alamri, *Neural. Comput. Appl.* **1**, 1 (2017)
[42] T Hayat, M Iqbal, H Yasmine, F E Alsaadi and H Gao, *Pramana J. Phys.* **85**(**1**), 125 (2015)
[43] T Hayat, M Waqas, S A Sehzad and A Alsaedi, *Pramana J. Phys.* **86**(**1**), 3 (2016)
[44] S Nadeem, R Mehmood and N S Akbar, *J. Magn. Magn. Mater.* **378**, 457 (2015)
[45] R K Bhatnagar, G Gupta and K R Rajagopal, *Int. J. Nonlinear Mech.* **30**(**3**), 391 (1995)